Modeling and Integration of Electric Vehicle Regenerative and Friction Braking for Motor/Dynamometer Test Bench Emulation

Article *in* IEEE Transactions on Vehicular Technology · January 2015

DOI: 10.1109/TVT.2015.2504363

CITATIONS
29

READS
667

4 authors, including:

Venkata Anand Kishore Prabhala
Missouri University of Science and Technology
15 PUBLICATIONS **247** CITATIONS

SEE PROFILE

Modeling and Integration of Electric Vehicle Regenerative and Friction Braking for Motor/Dynamometer Test Bench Emulation

P. Fajri, *Member, IEEE,* S. Lee, *Student Member, IEEE,* V. A. K. Prabhala, *Student Member, IEEE,* and M. Ferdowsi, *Member, IEEE*

***Abstract*— This paper provides a new approach for emulating electric vehicle (EV) braking performance on a motor/dynamometer test bench. The brake force distribution between regenerative braking and friction braking of both the front and rear axles are discussed in detail. A brake controller is designed, which represents a very close model of an actual EV braking system and takes into account both regenerative and friction braking limitations. The proposed brake controller is then integrated into the controller of an EV Hardware-in-the-Loop (HIL) test bench, and its performance is validated in real-time. The effect of adding the brake model is further investigated by comparing the experimental HIL energy consumption results to those obtained from ADvanced VehIcle SimulatOR (ADVISOR).**

***Index Terms*— Brake controller, electric vehicle (EV), friction braking, motor/dynamometer, regenerative braking.**

I. Introduction

Energy crisis, global warming, and environmental pollution have forced the developed countries to focus more progressively on a new generation of clean transportation. Electric vehicle (EV) technology, as a viable solution to clean transportation, is becoming the leading developmental trend of most major automotive companies. At the same time, extensive research is made towards the design and control of EV powertrain components to maximize performance, efficiency, and to extend the driving range of these vehicles. Research and advancement of this cutting edge technology and the need to obtain accurate predictions of powertrain performance, without the implications associated with manufacturing, has led to the use of Hardware-in-the-Loop (HIL) simulations. This method of emulation is considered a necessary tool in the study and implementation of EVs and allows for accurate verification and testing of developed control and energy management strategies. A number of articles in the literature have focused on EV emulation using HIL setups [1], [2]. Some previous works have focused on the comparison of different motors and energy analysis for electric drive vehicle concepts. Others have focused on evaluation of electric motor performance for different drive cycles [3], [4].

To accurately emulate the behavior of an EV on a test bench and provide a realistic model, all physical and performance characteristics of the vehicle should be considered. Performance characteristics of the vehicle such as electric motor power and torque ratings as well as braking capabilities of the vehicle play an important role in defining the limitations of different powertrain components and providing realistic emulation results. One inherent feature of EVs is regenerative braking [5]-[7]. The fundamental concept behind regenerative braking is recapturing the stored kinetic energy of the vehicle during braking [8]. This capability allows the electric motor to operate as a generator alongside friction braking and absorb excess energy while the vehicle is decelerating. Regenerative braking is an effective approach that improves vehicle efficiency, especially in heavy stop and go traffic [9].

The effect of vehicle braking and brake force distribution between regenerative and friction braking has been thoroughly studied in the literature and different simulation models have been proposed [7], [10]-[16]. Some experimental work has also been conducted on vehicle braking emulation using hardware setups [8], [17]-[21]. However, in most cases either the braking performance is tested on an actual vehicle or in the case of using a test bench, only the braking performance of the vehicle is studied and the interaction between braking and the overall vehicle performance is not considered. As a result, modeling EV braking system on a motor/dynamometer HIL test bench that also incorporates vehicle dynamics has not been considered before. Therefore, to provide a more realistic approach towards EV emulation, a need to integrate an accurate model of EV regenerative and friction braking into a HIL test bench control system is of great importance.

This paper extends the authors' previous research in [22] and [23] on emulating on-road operating conditions for EVs

P. Fajri is with the Department of Electrical and Computer Engineering, North Carolina State University, Raleigh, NC 27695 USA (e-mail: pfajri@ncsu.edu).

S. Lee is with LOTTE CHEMICAL, 115 Gajeongbuk-ro, Yuseong-gu, Daejeon, 305-726, Republic of Korea (e-mail: yr1mrcy@gmail.com).

V. A. K. Prabhala is with Infineon Technologies Americas Corp., El Segundo, CA 90245 USA (e-mail: vkpzvf@mst.edu).

M. Ferdowsi is a Professor with the Department of Electrical and Computer Engineering, Missouri University of Science and Technology, Rolla, MO 65409 USA (e-mail: Ferdowsi@mst.edu).

using a HIL motor/dynamometer setup. In the previous work, the behavior of an EV was emulated by calculating the resistive forces of an actual vehicle and controlling the motor/dynamometer set to evaluate EV performance for different scenarios. The current study provides a new approach for modeling and integration of EV braking system on the existing motor/dynamometer setup while taking into account the limitations imposed by friction and regenerative braking. The new model not only provides a comprehensive and more realistic approach towards emulating EV performance on a motor/dynamometer test bench, but can further be used in efficiency and energy consumption analysis studies related to these vehicles. Furthermore, the application of HIL simulation for friction and regenerative braking emulation is highlighted in this paper which can be used as an ideal platform to develop and verify different EV braking strategies.

This paper is organized as follows. In Section II, EV braking forces are explained. In Section III, the fundamentals of EV brake system design are discussed. Brake force distribution between the front and rear axles followed by proper distribution of brake force between the electric motor and friction braking is also explained in this Section. In Section IV, the HIL motor/dynamometer test bench structure for emulating EV performance is presented which is also used to implement the proposed braking model. A braking model is developed in Section V. The developed model is integrated into the controller of the existing HIL setup in Section VI and experimental results are presented in Section VII to validate its effectiveness. In Section VIII a case study is presented to highlight the importance of considering braking on vehicle energy analysis for HIL test bench studies. Finally, in Section IX, conclusions are drawn.

II. EV Braking Forces

The total braking force of an EV is made up of two terms; regenerative braking force of the electric motor, and friction braking force of the wheels. Regenerative braking is a key feature of EVs that allows the vehicle to recover significant amounts of energy during braking and store it in the energy storage system for future use. Energy recovery through regenerative braking is accomplished by controlling the electric motor to operate as a generator and converting the kinetic or potential energy of the vehicle's mass into electric energy [24]. In this case, only the driven axle is effective during regenerative braking.

During most heavy braking situations, the required braking force to decelerate, or stop the vehicle, is much greater than the resistive force produced by the electric motor. As a result, the majority of the braking energy must be absorbed by the friction brake system [25]. Therefore, in order to allow brake energy recovery while ensuring braking performance, both regenerative and friction braking have to coexist together [8].

III. Brake Force Distribution

One of the most important concerns affecting vehicle safety is the braking performance. The two fundamental design considerations for EV braking system are: (1) To quickly reduce the vehicle speed by applying sufficient braking force while maintaining the stability and controllability of the vehicle direction, and (2) To maximize the ability to recover as much braking energy as possible to improve the overall vehicle efficiency and therefore, extend the driving range. The former requires proper brake force distribution between the front and rear axles, while the latter requires a proper distribution of brake force between the electric motor and the friction braking system.

Advancement and development of new braking mechanisms such as electromechanical brakes (EMB) [26]-[28] have made it possible to implement and control brake force distribution. This braking system is also considered to be essential in the development of regenerative braking control for electric and hybrid electric vehicles [29]. The EMB technology uses an electric motor to generate braking force and compared to hydraulic brakes it allows accurate brake force control on each wheel [30].

A. Brake Force Distribution Between Front and Rear Axles

In order to achieve the shortest braking distance while ensuring maximum braking stability of the vehicle under various road conditions, proper allocation of the total braking force between the front and rear axle is essential. Not complying with this requirement will result in either the front or the rear wheels to lock sooner than expected and may lead to loss of stability or directional control. In the case where the rear wheels lock first, the vehicle will be prone to directional instability which can lead to loss of control. On the other hand, lockup of the front wheels does not cause directional instability but results in a loss of directional control which may be regained by partial release of the brakes [24].

In order for the front and rear wheels to obtain their maximum braking force, braking theory and design principles emphasize on distribution of total brake force between rear and front wheels in accordance with a nonlinear hyperbolic curve referred to as the ideal braking force distribution curve or *I* curve. This curve is calculated by considering the load transfer from the rear axle to the front axle during braking. Based on the vehicle body specifications this distribution is given by [31]

$$F_{bf} = \frac{-\sqrt{m^2 g^2 {L_a}^2 - 4mgh_g L F_{br}} - 2F_{br}h_g + mgL_a}{2h_g}, \quad 0 < \frac{F_{br}}{mg} < \frac{{L_a}^2}{4h_g L} \tag{1}$$

where m is the vehicle mass, L is the wheel base, h_g is the gravity center height of the vehicle, L_a is the length from the vehicle's center of gravity to the front axle, and F_{bf} and F_{br} are the braking forces acting on the front and rear wheels, respectively.

The resulting *I* curve is depicted in Fig. 1 for a typical vehicle. If the brake force distribution between the front and rear axle follows the ideal distribution curve, the front and rear

This article has been accepted for publication in a future issue of this journal, but has not been fully edited. Content may change prior to final publication. Citation information: DOI 10.1109/TVT.2015.2504363, IEEE Transactions on Vehicular Technology

wheels will be locked simultaneously and maximum brake performance and stability of the vehicle is achieved. If the ratio of the braking force is above the ideal curve, the rear wheels will be locked earlier than the front wheels. Otherwise, if the operating point falls below the ideal distribution curve, the front wheels will be locked prior to the rear wheels.

B. Brake Force Distribution Between Regenerative and Friction Braking

Another concern regarding EV brake system design is proper allocation of brake force between the friction brakes and the regenerative braking of the electric motor. In practice, regenerative braking should be applied to recapture as much energy as possible without compromising the vehicle stability and controllability. As far as EV driving and braking operations are concerned, the most important issue is safety [32]. Therefore, brake force control strategy and coordination of motor resistive torque with friction braking force plays an important role in both brake energy recovery and vehicle stability. Taking into account motor limitations and the fact that only the driven axle is effective during regenerative braking, the brake controller is responsible for balancing the regenerative and friction braking force. The brake controller is designed to maximize regenerative braking and to minimize the amount of kinetic energy lost to heat and friction.

When coordinating EV braking and calculating regenerative braking share, two main limitations should be considered. The first limitation is the maximum regenerative braking capability which is usually determined by the braking torque capability of the electric motor while operating as a generator [12]. This limitation affects maximum energy recovery during harsh deceleration of the vehicle. The other limitation which plays an important role particularly when considering efficiency and energy consumption is the inability of the electric motor to operate as a generator and charge the vehicle battery at low speeds. During deceleration, regenerative braking employs the back electromotive force (EMF) of the motor which can be considered as a voltage source to recharge the battery [20]. However, at low speeds due to the insufficient back EMF voltage generated by the electric motor, the regenerative braking process is no longer effective [8]. The low speed threshold depends on the type and specifications of the electric motor and the energy storage used within the vehicle. Although operating in regenerative mode at speeds below this threshold the electric motor is still capable of applying a resistive torque to slow down the vehicle, however, it is not capable of harvesting this energy. Hence, current is drawn from the energy storage resulting in further depletion of the vehicle energy storage system.

To more clearly analyze the effect of motor regenerative braking at low speeds an experiment was performed using a motor/dynamometer set. In this test the electric motor resembling the drive motor (DM) of the vehicle was connected to a bi-directional DC source and operated as a generator to emulate regenerative braking effect of a vehicle during deceleration. The DM was controlled to linearly reduce the shaft speed from 1750 rpm to a full stop. At the same time the dynamometer was controlled to provide a fixed torque of 50 Nm to represent the resistive forces acting on a vehicle as well as the inertial force of a moving vehicle during deceleration. It should be noted that calculating vehicle resistive forces is a more complex process discussed in section IV and cannot be considered constant for different speeds. However, for the sake of simplicity, this test was executed assuming a constant resistive force to show the DM regenerative braking capability during low speed operation. The results of this experiment are shown in Figs. 2 and 3. It can be seen that while the dynamometer is controlled to produce a constant torque, the

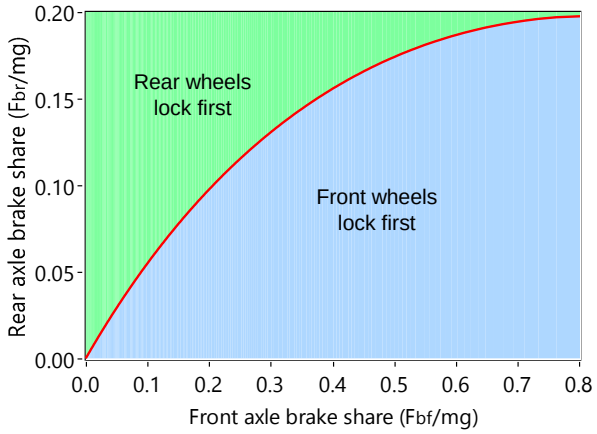

Fig. 1. Ideal brake force distribution curve on the front and rear axles of a typical vehicle

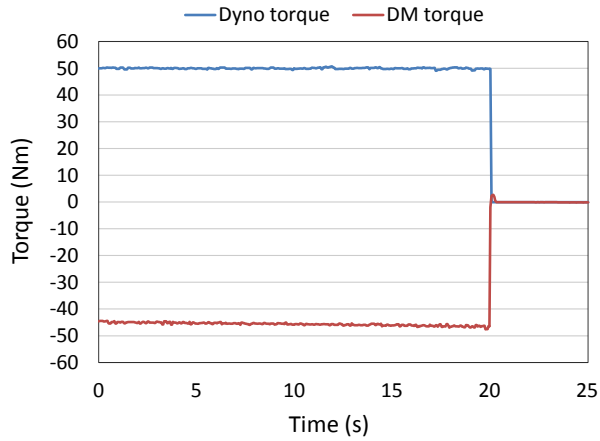

Fig. 2. Experimental results of DM and dynamometer generated torque

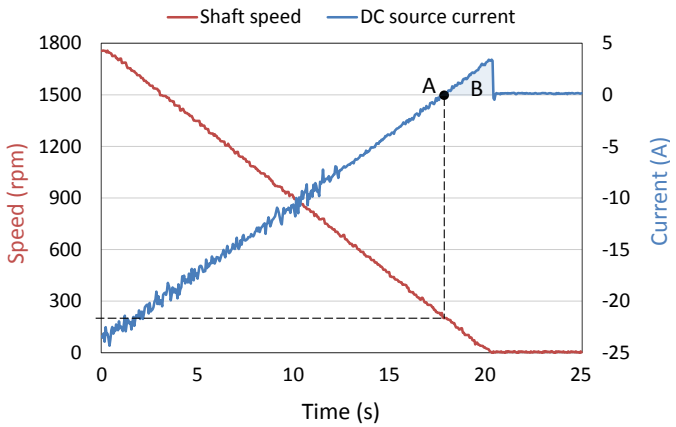

Fig. 3. Experimental results of shaft speed and DC source current variation

This article has been accepted for publication in a future issue of this journal, but has not been fully edited. Content may change prior to final publication. Citation information: DOI 10.1109/TVT.2015.2504363, IEEE Transactions on Vehicular Technology

DM reduces the shaft speed from 1750 rpm by producing an opposing torque. Fig. 3 shows that during this period the DM's DC current is negative until point A, indicating that current is being pushed back into the energy source. The shaft speed at point A is almost 200 rpm. However, at speeds below point A, positive current is drawn from the energy storage to resist the dynamometer torque and bring the shaft speed to zero. Assuming a fixed DC bus voltage throughout the simulation, the area below positive values of current (area B), represents energy loss during regenerative braking. This indicates that below a certain speed, regenerative braking is not capable of energy harvesting and can have a negative impact on the overall efficiency of the vehicle.

Although the energy loss during regenerative braking is small compared to the energy gained prior to point A, however, when longer driving times with frequent braking at lower speeds are considered, it would have a significant impact on energy consumption and range of the vehicle. As a result, in an actual EV, when the wheel speed is lower than a given threshold, braking is completely performed by the friction brakes and the electric motor is controlled to produce no braking force. The boundaries for maximum regenerative braking capability and low speed operation are shown in Fig. 4.

IV. EV Motor/Dynamometer Test Bench Structure

An EV test bench setup is typically composed of a DM coupled to a dynamometer through a common shaft. A controller is responsible for managing the interaction between the DM and the dynamometer electric motor under different driving scenarios, thus providing an accurate model of the actual vehicle under study. In most cases of vehicle emulation, the objective is to evaluate vehicle performance on a predetermined drive cycle. In this case, the aim is not only to follow the drive cycle profile but to control both motors in such a way that the contribution of torque from the dynamometer resembles the resistive forces acting on the actual vehicle, while simultaneously, the torque generated by the DM closely matches the DM torque of a real vehicle under different operating points. A block diagram representation of such system is depicted in Fig. 5.

The control block shown in Fig. 5 is responsible for calculating the speed and torque signals for each operating point. In this configuration, the reference speed is obtained from a predetermined drive cycle and is translated into a required rotational speed, which is then given to the DM through a PI controller that ensures accurate speed tracking. At the same time torque commands representing resistive forces acting on the vehicle are calculated within the controller and commanded to the dynamometer to emulate road load conditions. The controller is considered as one of the most important elements of a test bench, which must be capable of controlling both the DM and the dynamometer electric motor simultaneously under different driving scenarios. A block diagram representation of a controller previously developed by the authors' for this setup is depicted in Fig. 6.

As mentioned before, the controller block is responsible for calculating the speed reference for the DM and the resistive torque reference for the dynamometer. The required reference speed for the DM is calculated from the vehicle's translational speed by knowing the vehicle wheel radius (r_d) and total gear ratio (G) and is given by

$$\omega_{DM} = K_1 \frac{V_{ref}\ G}{r_d} \tag{2}$$

where K_1 is a constant for converting the translational speed of the vehicle from mile/h to m/s. The required dynamometer resistive torque (T_{Dyno}) is also calculated directly from the speed trace using the test bench and the vehicle dynamic

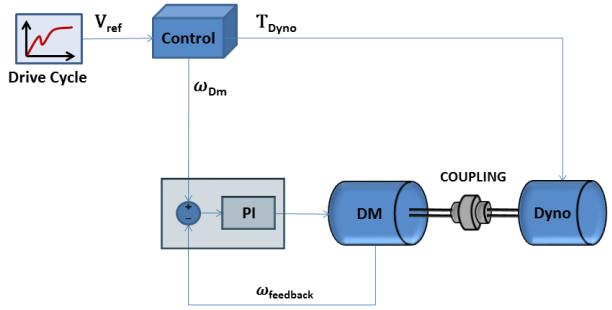

Fig. 5. Block diagram representation of the EV test bench [22]

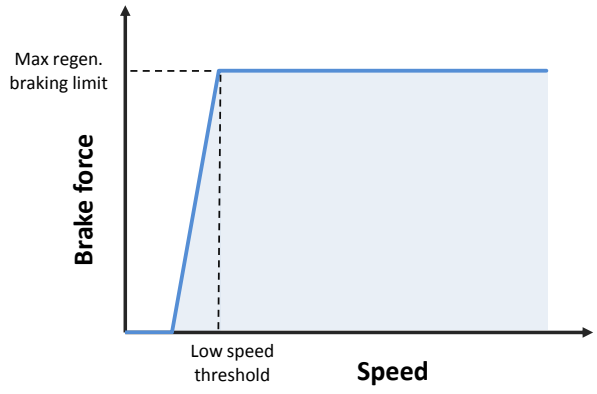

Fig. 4. Boundaries for regenerative braking capability

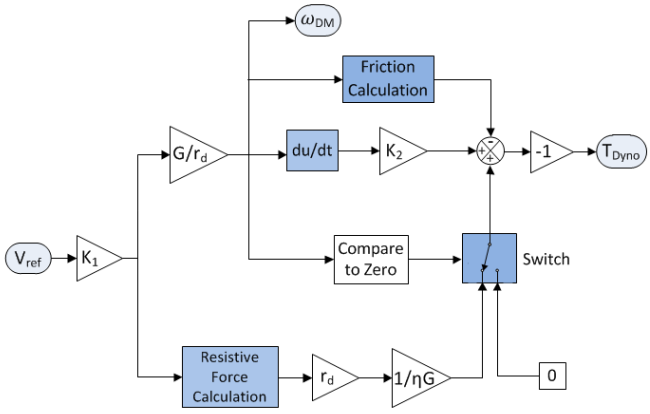

Fig. 6. Controller block for the EV test bench

equations at each instance and is given by [22]

$$T_{Dyno} = \frac{T_R}{\eta G} - \left(B_{DM} + B_{Dyno}\right)\omega_{Dm} + \left(\frac{J_{ew}}{\eta G^2} - J_{rotation}\right)\left(\frac{d\omega_{Dm}}{dt}\right) \quad (3)$$

where ω_{Dm} is the DM motor rotational speed, η represents the overall efficiency of the vehicle drive train to be emulated, $J_{rotation}$ is the rotating inertia of all the rotating components of the system, which includes the rotating inertia of the DM, dynamometer, and the coupling. In addition, B_{DM} and B_{Dyno} are the viscous coefficients of the DM and the dynamometer which represent friction losses. T_R is the total resistive torque calculated at the wheels, and is calculated from the resistive forces acting on the vehicle [23]. Knowing the vehicle specifications T_R is given by

$$T_R = r_d\left(mgf_r \cos\alpha + \frac{1}{2}\rho_a C_D A_f (V + V_w)^2 + mg\sin\alpha\right) \quad (4)$$

where m is the vehicle mass, fr is the rolling resistance coefficient, α is the ground slope angle, V is the vehicle speed in m/s, C_D is the aerodynamic drag coefficient that characterizes the shape of the vehicle's body, V_w is the wind speed on the vehicle's moving direction, A_f is the frontal area of the vehicle, and ρ_a is the mass density of air. J_{ew} in (3) represents the equivalent rotational inertia of the vehicle, which is discussed in detail in [33]. This term corresponds to the amount of flywheel inertia that has the same stored energy as a moving vehicle with a known mass when rotating at the same rotational speed as the vehicle's electric motor and is given by

$$J_{ew} = m(1 + 0.04 + 0.0025G^2){r_d}^2. \quad (5)$$

The experimental motor/dynamometer setup used both in [22] and in this paper is shown in Fig. 7. A block diagram representation of the experimental platform is also depicted in Fig. 8 which shows the interaction between the various subsystems as well as outlining the power and control signal for each component within the system. The experimental arrangement consists of a 15 kW, 6-pole permanent magnet synchronous motor (PMSM), which represents the DM. The PMSM shaft is connected to a 15 kW DC machine fed by a 4-quadrant chopper acting as the dynamometer to emulate road load, vehicle inertia, and friction braking force.

The PMSM drive is connected to a high power bi-directional DC source representing vehicle energy storage system. The DC source is equipped with full regenerative capability allowing it to absorb energy during regenerative braking operation of the PMSM. LabVIEW software is used to perform real-time simulation by building the vehicle model and executing the commands in real-time using an on-board PC processor. To emulate on-road operation conditions, speed and torque commands are calculated in real-time from the mathematical models of vehicle dynamics and road load

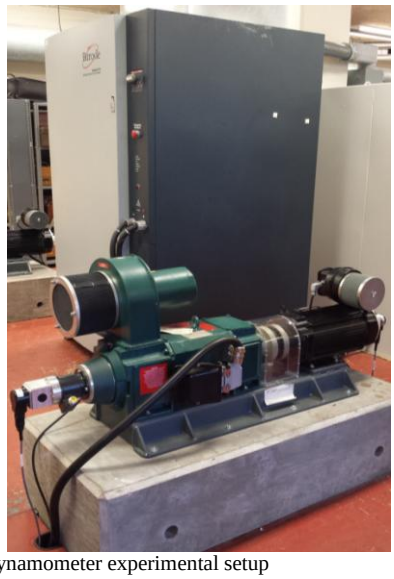

Fig. 7. Motor/dynamometer experimental setup

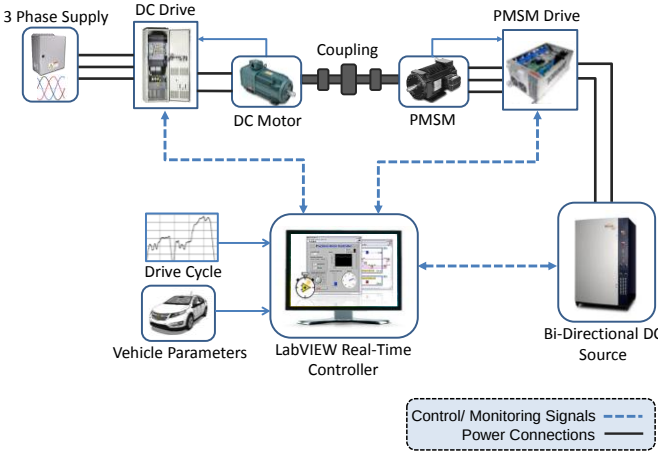

Fig. 8. Block diagram representation of the experimental setup

according to (2) and (3). The LabVIEW real-time controller then changes the operating point of the dynamometer and the DM continuously and sends synchronous speed and torque signals to the two drives at each instance allowing exact interaction between them. The need of a real-time communication is satisfied by means of a Controller Area Network (CAN) bus which assures synchronous distribution of reference speed and torque commands. CAN communication also enables real-time monitoring of system critical signals such as the actual speed and torque of both electric motors as well as the voltage and current of the DC source. With the CAN bus data rate set at 500 kbps, a 10ms update rate is achieved to command and monitor all variables.

V. Decision Logic of Brake Controller

In order to accurately emulate EV braking performance on a motor/dynamometer HIL setup, first the braking control strategy should be defined so that it represents a very close model of an actual EV braking system. In this paper, a front

This article has been accepted for publication in a future issue of this journal, but has not been fully edited. Content may change prior to final publication. Citation information: DOI 10.1109/TVT.2015.2504363, IEEE Transactions on Vehicular Technology

wheel-drive configuration is considered. As a result the braking forces on the front axle consist of motor regenerative braking as well as front wheel friction brakes, while the rear axle braking force only consists of rear wheel friction brakes.

Since the EV HIL setup under study is designed to follow a standard drive cycle, the required DM torque can be calculated from the vehicle and test bench dynamic equations at each instance [23]. Based on the control model of Fig. 6, the desired DM torque to ensure accurate speed tracking is given by

$$T_{DM} = \frac{J_{ew}}{\eta G^2}\left(\frac{d\omega_m}{dt}\right) + \frac{T_R}{\eta G}. \quad (6)$$

The calculated DM torque from (6) is used as an input reference to the brake controller. As long as this torque is positive, the brake controller is inactive. As soon as the calculated DM torque is negative the brake controller calculates the required braking torque on the front and rear axles according to the ideal braking curve distribution. It should be noted that the brake torque distribution follows the same trend as the brake force distribution given in (1) and brake torque and force are related to each other by vehicle wheel radius. As long as the front axle's share is within the motor capabilities and the motor speed is above the low speed threshold, the front axle's share of the braking force is met solely by the DM. At speeds below the threshold, the brake controller gradually decreases the regenerative braking share of the DM and at the same time, increases the friction braking share of the front wheels. A flowchart representation of the brake controller is shown in Fig. 9.

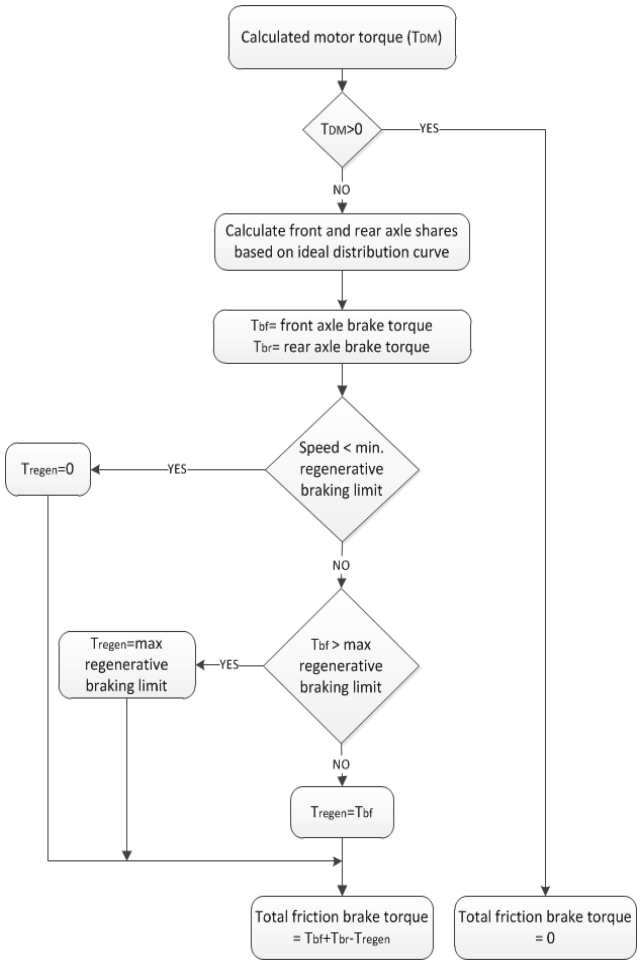

Fig. 9. Flow chart representation of the brake controller

VI. Integration of the Braking Control Strategy into HIL Setup

The proposed controller for the motor/dynamometer test bench platform shown in Fig. 6 does not take into account the effect of friction braking. In this model, it is assumed that the only means of deceleration is the regenerative braking force of the DM. Also, there are no limitations on the regenerative braking capabilities of the DM. In order to consider the effect of friction brakes and present a comprehensive EV emulation controller suitable for any motor/dynamometer test bench, the brake controller of Fig. 9 is integrated into the previous EV HIL controller. This is achieved by subtracting the total friction braking term, calculated by the brake controller, from the original dynamometer torque reference (T_{Dyno}). The reason for this is that during deceleration and in regenerative braking mode, the DM is providing opposing torque to reduce the shaft speed, which is proportional to the vehicle speed. At the same time, the dynamometer is controlled to provide a torque in positive alignment with the shaft rotational direction, hence, emulating the available kinetic energy of the vehicle and assisting vehicle movement. As a result, since friction brake force is also considered as a resistive force opposing vehicle movement, friction braking effect can be realized by subtracting the calculated friction braking torque from the torque produced by the dynamometer during deceleration. Therefore, after the brake controller calculates the required friction braking on the rear and front axles with regards to the ideal braking curve and motor regenerative braking capabilities, the sum of the front and rear axle friction braking is subtracted from the original dynamometer torque command. The complete motor/dynamometer controller block diagram containing the brake controller block is shown in Fig. 10.

VII. Experimental Results and Validation

To verify the overall performance of the system and validate the effectiveness of the implemented control approach, while showing the application of HIL in emulating EV friction and regenerative braking capabilities, two experiments were conducted using the HIL experimental setup of Fig. 7. The vehicle and test bench parameters used for both tests are presented in Table I. Each test was performed for the duration of 510 seconds of the Urban Dynamometer Driving Schedule (UDDS). The first test was performed using the original control model of Fig. 6 without taking into account the friction braking effect. The results for this case are illustrated in Fig. 11. The second test was executed considering the brake distribution between regenerative braking and friction braking of the front and rear axles and using the modified control block diagram of Fig. 10. For this

This article has been accepted for publication in a future issue of this journal, but has not been fully edited. Content may change prior to final publication. Citation information: DOI 10.1109/TVT.2015.2504363, IEEE Transactions on Vehicular Technology

TABLE I
Vehicle and Test-Bench Specifications

Parameter	Value
Vehicle mass (m)	600 kg
Air density (ρ_a)	1.22 kg/m^3
Aerodynamic drag coefficient (C_d)	0.3
Frontal area (A_f)	1.6 m^2
Rolling resistance coefficient (fr)	0.01
Wheel radius (r_d)	0.28 m
Overall gear ratio (G)	2.6
Inertia of all the rotating components ($J_{rotation}$)	0.038 kg.m^2
Equivalent Vehicle Rotational Inertia (J_{ew})	49.72 kg.m^2
Vehicle drive train overall efficiency (η)	%95
DM viscous coefficient (B_{DM})	0.0086 N.m/(rad/s)
DM power capability (Nominal/Maximum)	15 kW/ 36 kW
Dynamometer viscous coefficient (B_{Dyno})	0.0133 N.m/(rad/s)
Dynamometer power capability (Nominal/Maximum)	15 kW/ 30 kW
Distance from center of gravity to front wheel (L_a)	0.95 m
Gravity center height (h_g)	0.5 m
Wheel base (L)	2.2 m

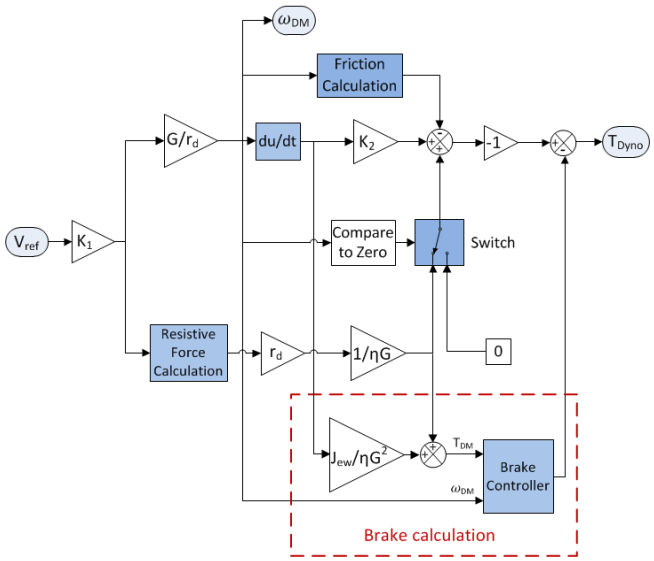

Fig. 10. Modified control block for the EV test bench

case, the maximum regenerative braking limit was assumed to be -50 Nm and the motor low speed limit was chosen to be 200 rpm based on the DM specifications. The experimental results for this case are illustrated in Fig. 12.

Comparing the results from Figs. 11(a) and 12(a), it can be seen that for both cases the vehicle follows the drive cycle precisely and only minor speed variations from the reference speed exist. From Fig. 11(b), it is concluded that the required maximum DM regenerative torque to meet the drive cycle deceleration needs is approximately −86 Nm for this vehicle. However, as seen in Fig. 12(b), it is clear that due to the presence of the brake controller, the distribution of friction braking and regenerative braking is controlled such that the motor regenerative braking torque is limited to the preset value of −50 Nm. The DM regenerative braking torque and total friction braking share of both axles are shown in Figs. 13 and 14. These results show the effectiveness of the brake

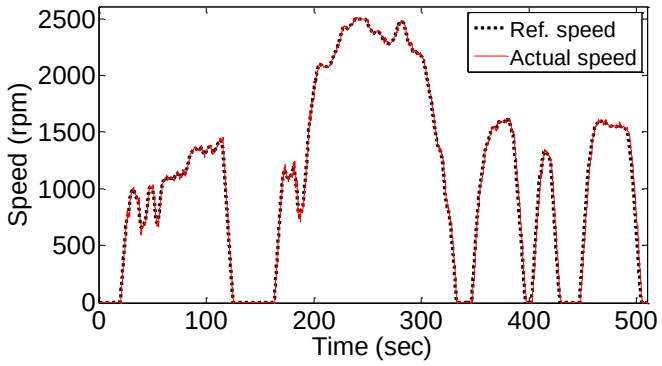

(a)

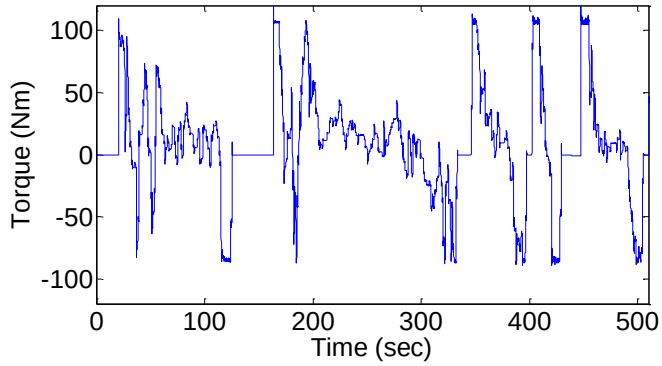

(b)

Fig. 11. Experimental results without the brake controller (a) Reference and actual DM speed (b) DM torque

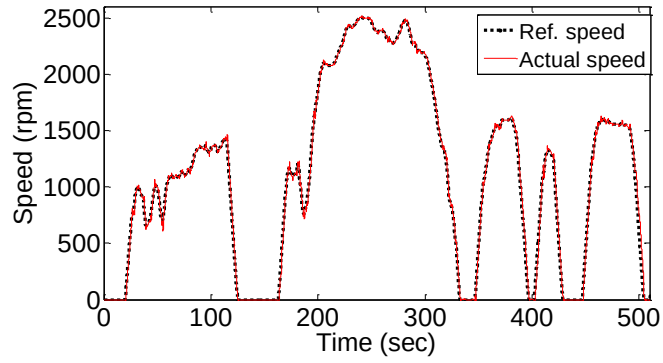

(a)

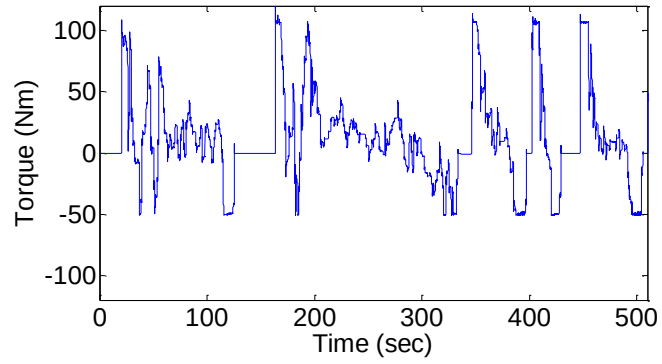

(b)

Fig. 12. Experimental results with the implemented brake controller (a) Reference and actual DM speed (b) DM torque

controller in accurately allocating the required brake power between friction and regenerative braking. It is observed that while the DM regenerative torque is limited to −50 Nm, for values more than this limit, total friction brake torque is used to meet the drive cycle deceleration needs. The friction braking share of each axle is also shown in Figs. 15 and 16. A closer look into the results of Figs. 13 through 16 reveals that for values below the regenerative limit, the front axle's friction braking share is zero and all the braking requirement of the front axle is met by regenerative braking. However, as soon as the regenerative braking torque exceeds its higher limit, the front axle friction braking is used to assist with the deceleration process and meet vehicle's braking requirements. It is also noted from Figs. 15 and 16 that the front axle's share of friction braking is slightly lower than the rear axle's share due to the regenerative braking effect of the DM on the front axle.

VIII. Case Study Showing the Importance of Considering Brake Allocation on Energy Consumption

To further analyze the effect of considering braking allocation on energy consumption, two cases of EV emulation discussed in section VII were compared to the results obtained from the ADvanced VehIcle SimulatOR (ADVISOR). For this comparison a full UDDS drive cycle was considered and once again the vehicle and test bench parameters were assumed to be the same as those given in Table I. Given the significant advantage of ADVISOR in using MATLAB/Simulink environment, and the flexibility of changing the parameters, the ADVISOR vehicle and regenerative braking parameters were chosen to closely resemble those used in the experimental setup.

To measure the energy consumption for each experimental case, current and voltage measurements from the DC source connected to the PMSM were recorded in real-time. The final results of energy consumed, recovered, and lost to friction braking throughout the drive cycle are presented in Table II for each case. The total energy consumed from the source is calculated by integrating the positive values of power over the full drive cycle. The consumed energy represents the required energy to propel the vehicle and does not take into account the energy recovered from regenerative braking. Similarly the energy recovered through regenerative braking was calculated from integration of the negative values of power over the complete drive cycle. Also, the energy lost to friction for the case with the braking model was calculated from the real-time brake torque command given to the dynamometer with respect to vehicle speed.

Comparing the results of consumed energy reveals that the ADVISOR simulation result is closer to the result obtained from the experimental case with brake modeling. On the other hand, the consumed energy for the case with no braking is relatively higher compared to the other two cases. This difference is mainly due to the extra current being drawn from the source during low speed regenerative braking discussed in section III (b) which adds up to the total consumption. As for the energy recovered through regenerative braking, it is clear that the regenerative braking energy obtained from the

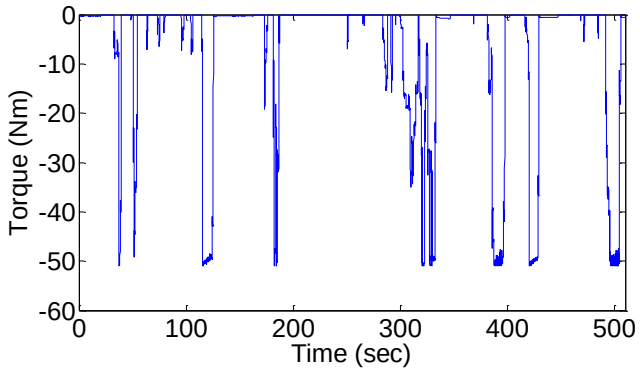

Fig. 13. DM regenerative braking share

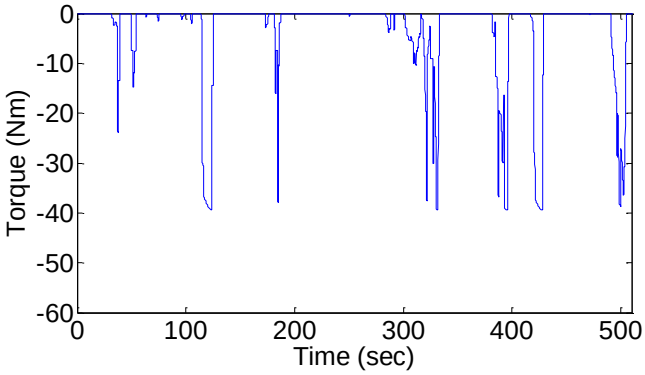

Fig. 14. Total friction braking share

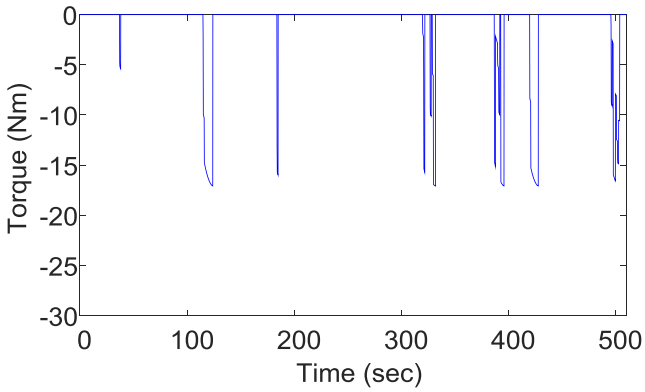

Fig. 15. Front axle share of friction brake

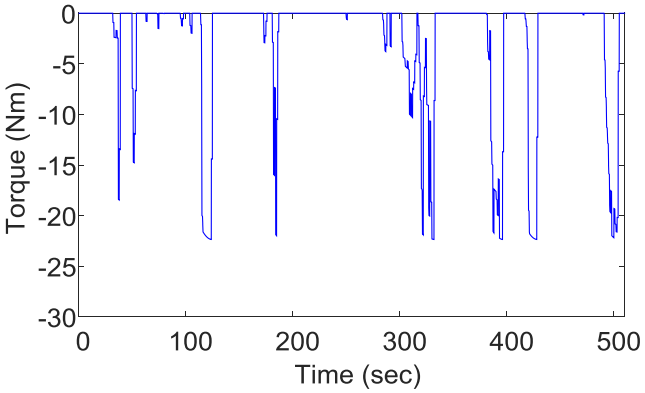

Fig. 16. Rear axle share of friction brake

TABLE II
Energy Results for the UDDS Drive Cycle

CASE / ENERGY DISTRIBUTION	Experimental		Simulation
	Case I	Case II	Case III
	Without brake modeling	With brake modeling	ADVISOR
Consumed energy (Wh)	856.3	852.5	851.1
Recovered energy through regenerative braking (Wh)	-226.2	-145.1	-139.2
Net energy consumption (Wh)	630.1	707.4	711.9
Energy lost to friction (Wh)	0	-90.1	-94.5

experimental case with the brake model is once again very close to the result obtained from ADVISOR. For both these cases the recovered energy is almost 17% of their total consumed energy. However, as expected, the total energy recovered during braking for the case without the brake model (case I) is significantly higher and accounts for almost 26% of its consumed energy. This is due to the fact that in the absence of friction braking, the DM is the only means of reducing the speed. As such it is sometimes forced to generate very high regenerative braking force to fulfill the deceleration requirements of the drive cycle, resulting in more energy recovery. However, since the brake force distribution requirements are not considered, the simulation is far from realistic. The high regenerative braking energy recovery for case I can also be justified from the results of energy lost to friction. Considering that the energy lost to friction is no longer available for recovery, the results show no friction losses in the absence of a braking model, whereas a relatively high friction loss is recorded for the other two cases.

In Table II the net energy consumption is calculated from the difference between the absolute values of consumed energy and the recovered energy from regenerative braking. This value corresponds to the total energy required to complete the drive cycle and is considered as a crucial parameter when estimating the range of an EV with respect to its energy storage capacity. Comparing the results of the net consumption obtained from ADVISOR with each experimental case shows an error of 11.5% for case I and 0.6% for case II. This notable difference indicates that by implementing a braking model that represents a close model of an actual EV braking system, very accurate HIL test bench results could be achieved. Whereas not considering a braking model could result in significant errors that can lead to unrealistic results. This can also be concluded by comparing the results of other parameters from Table II between the experimental cases and the results obtained from ADVISOR.

IX. Conclusion

A new approach for emulating EV braking performance on a motor/dynamometer test bench was proposed. This was achieved by introducing a brake controller which takes into account brake force distribution between regenerative and friction braking. To validate the effectiveness of this approach, experiments with and without the brake controller were conducted using a motor/dynamometer HIL experimental setup. The experimental results confirmed the desired operation of the brake controller in distributing the required brake force between regenerative and friction braking without impairing the overall system performance. It was also concluded that from the perspective of energy consumption, considering braking limitations provides a more realistic approach towards EV emulation on a motor/dynamometer setup and allows for a more accurate assessment of EV performance. Using this approach for HIL implementation of EV braking performance facilitates further research focused on the development of different EV braking strategies. These studies can lead to further efficiency improvement of these vehicles through better use of regenerative braking capability.

References

[1] S. Jeschke, H. Hirsch, M. Koppers, and D. Schramm, "HIL Simulation of electric vehicles in different usage scenarios," in *Proc. IEEE Electric Vehicle Conference (IEVC)*, Greenville, SC, March 4-8, 2012, pp. 1-8.

[2] R. M. Schupbach and J. C. Balda, "A versatile laboratory test bench for developing powertrains of electric vehicles," *IEEE 55th Vehicular Technology Conference*, 2002, pp. 1666–1670.

[3] C. Oh, "Evaluation of motor characteristics for hybrid electric vehicles using the Hardware in-the-Loop concept," *IEEE Trans. Veh. Technol.*, vol. 54, no. 3, pp. 817-824, May 2005.

[4] S. Oh and A. Emadi, "Test and simulation of axial flux motor characteristics for hybrid electric vehicles," *IEEE Trans. Veh. Technol.*, vol. 53, no. 3, pp. 912–919, May 2004.

[5] X. Nian, F. Peng, and H. Zhang, "Regenerative Braking System of Electric Vehicle Driven by Brushless DC Motor," *IEEE Trans. Ind. Electron.*, vol. 61, no. 10, pp. 5798- 5808, Jan. 2014.

[6] D. Kim, S. Hwang, and H. Kim., "Vehicle Stability Enhancement of Four-Wheel-Drive Hybrid Electric Vehicle Using Rear Motor Control," *IEEE Trans. Veh. Technol.*, vol. 57, no. 2, pp. 727- 735, 2008.

[7] F. Wyczalek, and T. Wang, "Regenerative Braking Concepts for Electric Vehicles - A Primer," *SAE Technical Paper* 920648, 1992, doi:10.4271/920648.

[8] P. Suntharalingam, "Kinetic energy recovery and power management for hybrid electric vehicles," Ph.D. dissertation, Department of Engineering & Applied Science, Cranfield University, 2011.

[9] H. Yeo, D. Kim, S. Hwang, and H. Kim, "Regenerative braking algorithm for a HEV with CVT ratio control during deceleration," In *Proc. of SAE CVT Congress*. 2004.

[10] B. Cao, Z. Bai, and W. Zhang, "Research on control for regenerative braking of electric vehicle," in *Proc. IEEE International Conference on Vehicular Electronics and Safety*, Shaan'xi, China, Oct. 14-16, 2005, pp. 92-97.

[11] J. Guo, J. Wang, and B. Cao, "Regenerative braking strategy for electric vehicles," in *Proc. IEEE Intelligent Vehicles Symposium*, Xi'an , China, June 3-5, 2009, pp. 864-868.

[12] L. Chu, et al., "Integrative braking control system for electric vehicles," in *Proc. IEEE Vehicle Power and Propulsion Conference (VPPC)*, Chicago, IL, Sept. 6-9, 2011, pp. 1-5.

[13] Z. Ling and T. Lan, "Braking force distribution research in electric vehicle regenerative braking strategy," in *Proc. IEEE Computational Intelligence and Design (ISCID)*, Hangzhou, China, Oct. 28-29, 2012, pp. 98-101.

[14] G. Jinfang, et al., "The coordinated control of motor regenerative braking torques defined by accelerator pedal and brake pedal of electric vehicle," in *Proc. IEEE Vehicle Power and Propulsion Conference (VPPC)*, Seoul, South Korea, Oct. 9-12, 2012, pp. 119-123.

[15] J. Ko, S. Ko, I. Kim, D. Hyun, and H. Kim, "Co-operative Control for Regenerative Braking and Friction Braking to Increase Energy Recovery without Wheel Lock," *Int. J. Automot. Technol.*, vol. 15, no. 2, pp. 253-262, 2014.

[16] D. Kim and H. Kim, "Vehicle stability control with regenerative braking and brake force distribution for a four-wheel drive hybrid electric vehicle," *Proceedings of the Institution of Mechanical Engineers, Part D: Journal of Automobile Engineering*, vol. 220, no. 6, pp. 683–693, 2006.

[17] J. Ko, et al., "Development of a co-operative control algorithm during regenerative braking for a fuel cell electric vehicle," in *Proc. IEEE Vehicle Power and Propulsion Conference (VPPC)*, Chicago, IL, Sept. 6-9, 2011, pp. 1-6.

[18] H. Fujimoto, et al., "Field and bench test evaluation of range extension control system for electric vehicles based on front and rear driving-braking force distributions," in *Proc. IEEE Power Electronics Conference (IPEC)*, Hiroshima, Japan, May 18-21, 2014, pp. 1671-1678.

[19] J. Ko, S. Ko, H. Son, B. Yoo, J. Cheon, and H. Kim, "Development of Brake System and Regenerative Braking Co-operative Control Algorithm for Automatic Transmission-based Hybrid Electric Vehicle," *IEEE Trans. Veh. Technol.*, IEEE early access articles, 2014.

[20] M. J. Yang, H. L. Jhou, B. Y. Ma, and K. K. Shyu, "A cost-effective method of electric brake with energy regeneration for electric vehicles," *IEEE Trans. Ind. Electron*., vol. 56, no. 6, pp. 2203–2212, Jun. 2009

[21] H. Yeo and H. Kim, "Hardware-in-the-Loop Simulation of Regenerative Braking for a Hybrid Electric Vehicle," *Journal of Automobile Engineering*, vol. 216, pp. 855-864, 2002.

[22] P. Fajri, R. Ahmadi, and M. Ferdowsi, "Control approach based on equivalent vehicle rotational inertia suitable for motor-dynamometer test bench emulation of electric vehicles," in *Proc. IEEE International Electric Machines and Drives Conference (IEMDC)*, Chicago, IL, May 12-15, 2013, pp. 1155 - 1159.

[23] P. Fajri, R. Ahmadi, and M. Ferdowsi, "Test Bench for Emulating Electric Drive Vehicle System Using Equivalent Vehicle Rotational Inertia," in *Proc. IEEE Power and Energy Conference at Illinois (PECI)*, Champaign, IL, Feb. 22-23, 2013, pp. 83 - 87.

[24] M. Ehsani, Y. Gao, S. E. Gay, and A. Emadi, Modern Electric, Hybrid Electric, and Fuel Cell Vehicles: Fundamentals, Theory, and Design. Boca Raton, FL: CRC, Dec. 2004.

[25] Y. Gao, L. Chen, and M. Ehsani, "Investigation of the effectiveness of regenerative braking for EV and HEV," *SAE transactions* 108.6; PART 2 (2000): 3184-3190.

[26] C. Maron, T. Dieckmann, S. Hauck, and H. Prinzler, "Electromechanical brake system: Actuator control development system," *SAE Technical Paper* 970814, 1997, doi:10.4271/970814.

[27] W. Xiang, P. C. Richardson, C. Zhao, and S. Mohammad. "Automobile brake-by-wire control system design and analysis," *IEEE Trans. Veh. Technol., vol.* 57, no. 1, pp.138-145, Jan. 2008.

[28] J. Cheon, "Brake By Wire System Configuration and Functions using Front EWB (Electric Wedge Brake) and Rear EMB (Electric-Mechanical Brake) Actuators," *SAE Technical Paper* 2010-01-1708, 2010, doi:10.4271/2010-01-1708..

[29] J. Ahn, K. Jung, D. Kim, H. Jin, H. Kim, and S. Hwang, "Analysis of a regenerative braking system for hybrid electric vehicles using an electromechanical brake," *Int. J. Automotive Technol.*, vol. 10, no. 2, pp. 229– 234, Apr. 2009.

[30] C. Jo, S. Hwang, and H. Kim, "Clamping-Force Control for Electromechanical Brake," *IEEE Trans. Veh. Technol.*, vol. 59, no. 7, pp. 3205-3212, 2010.

[31] N. Mutoh and Y. Nakano, "Dynamics of front-and-rear-wheel-independent- drive-type electric vehicles at the time of failure," *IEEE Trans. Ind. Electron.*, vol. 59, no. 3, pp. 1488–1499, Mar. 2012.

[32] N. Mutoh, Y. Hayano, H. Yahagi, and K. Takita, "Electric braking control methods for electric vehicles with independently driven front and rear wheels," *IEEE Trans. Ind. Electron*., vol. 54, no. 2, pp. 1168–1176, Apr. 2007

[33] P. Fajri, R. Ahmadi, and M. Ferdowsi, "Equivalent vehicle rotational inertia used for electric vehicle test bench dynamic studies," in *Proc. 38th IEEE Industrial Electronics Society Annual Conference*, Montreal, Canada, Oct. 25-28, 2012, pp. 4115 - 4120.

Poria Fajri (S'13–M'15) received the B.S. degree in electronics from Urmia University, Urmia, Iran, in 2005, the M.S. degree in electrical engineering from the University of Tehran, Tehran, Iran, in 2008, and the Ph.D. degree in electrical engineering from Missouri University of Science and Technology, Rolla, MO, USA, in 2014. Currently, he is a Postdoctoral Research Associate with the NSF FREEDM Systems Center, North Carolina State University, Raleigh, NC, USA. His research interests include electric-drive vehicles, renewable energy systems, Flexible AC Transmission Systems (FACTS), and power electronic converters.

Sangin Lee (S'10) was born on March 14, 1981 in Korea. He received the B.S. degree in Electrical and Computer Engineering and the M.S. degree in Electrical Engineering from Hanyang University, Seoul, Korea, in February 2007 and February 2009, respectively. He received the Ph.D. degree in Electrical Engineering from the Missouri University of Science and Technology in July 2015. After the graduation, he joined LOTTE CHEMICAL which is located in Daejeon, Korea. His research interests include multilevel converters and inverters, LLC resonant converters, unity power factor control, and LCL filter control. Currently, as his company produces Zn-Br_2 Redox Flow Batteries, his job is to design grid tied converters and inverters.

Venkata Anand Kishore Prabhala (S'14) received the B.S. degree from National Institute of Technology, Warangal, India, in 2005, and the M.S. and Ph.D. degrees from Missouri University of Science and Technology, Rolla, USA, in 2010 and 2014, respectively. From 2005 to 2008, he was a Project Engineer at Larsen & Toubro Ltd., India. Since 2014, he has been a Global Rotation Engineer at Infineon Technologies Americas Corp., El Segundo, CA, USA. His research interests include design and control of power electronic converters, ac and dc microgrids, electric drive vehicles, and renewable energy systems.

Mehdi Ferdowsi (S'02–M'04) received the B.S. degree in electronics from the University of Tehran, Tehran, Iran in 1996, the M.S. degree in electronics from Sharif University of Technology, Tehran, in 1999, and the Ph.D. degree in electrical engineering from the Illinois Institute of Technology, Chicago, in 2004. He joined the faculty of the Missouri University of Science and Technology, Rolla, in August 2004, where he is currently a Professor in the Electrical and Computer Engineering Department. His research interests are in the areas of power electronics, energy storage, smart grid, vehicular technology, and wide bandgap devices. Dr. Ferdowsi received a Missouri S&T Outstanding Teaching Award in the 2005-2006 academic year. He was a recipient of a National Science Foundation CAREER Award in 2007. Dr. Ferdowsi and his students won a best paper award at the IEEE Vehicle Power and Propulsion Conference in 2008. He is an Associate Editor of the IEEE TRANSACTIONS ON POWER ELECTRONICS.